

08.2

Low-temperature growth of InAs nanowires and nanosheets on Si(100) substrates

© A.A. Koryakin^{1,2}, E.V. Ubyivovk¹, K.P. Kotlyar^{1–3}, V.V. Lendyashova^{1,2}, R.R. Reznik¹, G.E. Cirilin^{1–3}

¹ St. Petersburg State University, St. Petersburg, Russia

² Alferov Federal State Budgetary Institution of Higher Education and Science, Saint Petersburg National Research Academic University of the Russian Academy of Sciences, St. Petersburg, Russia

³ Institute of Analytical Instrument Making, Russian Academy of Sciences, St. Petersburg, Russia

E-mail: koryakinaa@spbau.ru

Received September 27, 2023

Revised September 27, 2023

Accepted December 18, 2023

The results of the study of low-temperature growth of InAs nanowires and nanosheets on Si(100) substrates by molecular beam epitaxy are presented. The morphology and structure of nanowires and nanosheets were studied by scanning and transmission electron microscopy. It was found that, during the growth of nanowires in the [110] direction, the interface between the catalyst and nanowire contains two facets: InAs(11 $\bar{1}$) and InAs(111). A simple geometrical model of the nanowire growth has been proposed to explain the stability of these facets, and estimates for the ratio between step velocities on these facets have been obtained.

Keywords: nanowires, nanosheets, vapor–solid–solid growth mechanism, A^{III}B^V semiconductors

DOI: 10.61011/PJTF.2024.07.57466.19742

Recently, the study of low-temperature growth of A^{III}B^V nanowires and nanosheets via the vapor–solid–solid (VSS) mechanism has attracted much attention from researchers [1–3]. Low-temperature growth of A^{III}B^V nanostructures via the VSS mechanism is performed by molecular beam epitaxy (MBE) and metalorganic vapour-phase epitaxy at temperatures significantly lower than the catalyst eutectic temperature at which the catalyst particle is solid. For instance, the process of growing InAs nanowires (NWs) under the VSS mechanism proceeds at the temperatures of $\sim 300^\circ\text{C}$, while the eutectic temperature of the Au–In catalyst is 453.3°C [4]. An increased interest in this growth mechanism is caused by that the VSS growth exhibits a number of advantages over the more common synthesis method obeying the vapor–liquid–solid (VLS) mechanism [1,2]. Among the VSS mechanism advantages there are a more comprehensive control of the nanocrystal (zinc blende/wurtzite) crystalline phase and possibility to create sharp axial heterojunctions by switching both the group V and group III fluxes (due to the absence of the so-called „reservoir effect“ [2]). In addition, low growth temperatures open up new ways to integrate A^{III}B^V semiconductors with silicon electronics. Despite a relatively large number of publications on this topic, the VSS growth of A^{III}B^V nanostructures on silicon substrates has not received enough attention. This work was devoted to studying the VSS growth of InAs nanostructures on Si(100) substrates; we continued the studies of the low-temperature growth of A^{III}B^V NWs described in papers [5,6] where the VSS growth of InAs(P) NWs on Si(111) substrates was demonstrated. Growth on Si(100) substrates is of particular

interest for studying the mechanisms of VSS-growth of InAs, since these substrates have no preferable growth direction, while in the case of a (111) substrate the preferable direction is $[\bar{1}\bar{1}\bar{1}]/[111]$. As a result, conditions for growing nanostructures in various crystallographic directions get created.

The InAs structure was grown by MBE at a Riber Compact 21 setup equipped with a separate metallization chamber for depositing the catalyst (gold) without breaking vacuum conditions. As the substrates, *p*-doped Si(100) wafers with the 2° misorientation in the [011] direction were used. Gold was deposited at 550°C for 50 s with subsequent 1 min exposure at the same temperature. The substrate metallization was preceded by conventional cleaning in the hydrofluoric acid aqueous solution and annealing at 850°C . After transferring the substrate into the growth chamber, the growth temperature was set to 270°C . Growth of InAs was initiated by simultaneously opening the indium and arsenic shutters and was continued for 15 min. Morphological and structural properties of the obtained samples were studied by scanning electron microscopy (SEM) and transmission electron microscopy (TEM) (Figs. 1 and 2). The research results confirmed the formation of nanostructures of various morphologies, including nanowires and nanosheets (Fig. 1). In their turn, catalyst particles were observed in high-resolution TEM images at the tops of nanostructures. Low values of the growth temperatures, as well as the composition of the catalyst particles Au–In (20–25 at.% indium) determined by energy-dispersive X-ray spectroscopy, make us to unambiguously conclude that the nanostructures have been grown under the VSS mechanism. Notice that

the growth on Si(111) substrates under similar deposition conditions typically results in formation of nanostructures of only one type, namely InAs NWs growing in the $[000\bar{1}]$ direction [6]. In our case, various types of nanostructures are observed on the Si(100) substrate surface (Figs. 1, *a* and *b*).

1. NWs growing in the InAs $[000\bar{1}]$ direction and having the length of $1\text{--}4\ \mu\text{m}$ and constant diameter of about 10 nm. The catalyst–NW interface is perpendicular to the crystal growth direction. These NWs grow in four directions $[111]$ and $[\bar{1}\bar{1}\bar{1}]$ relative to the substrate and have the wurtzite crystal structure. In this case, TEM data completely reproduce the results of [6] where the growth of InAs NWs on Si(111) substrates was studied.

2. Nanosheets about $1\ \mu\text{m}$ in length and $\sim 100\ \text{nm}$ in lateral size having the wurtzite structure (the diffraction pattern is presented in the inset to Fig. 2, *a*). The catalyst–NW InAs(0001)/(000 $\bar{1}$) interface is inclined at the angle of $\sim 40^\circ$ to the growth direction (Fig. 2, *a*) [1].

3. NWs about $1\ \mu\text{m}$ long growing in the InAs $[110]$ direction and having the zinc blende structure (the diffraction pattern is given in the inset to Fig. 2, *b*). Their diameter decreases from base to top and amounts to $\sim 10\text{--}30\ \text{nm}$ [7]. The catalyst–NW interface is not flat (Fig. 2, *b*).

4. Nanostructures formed as a result of the catalyst particle instability and NW transformation into a nanosheet (see the inset to Fig. 1, *b*) [8].

The listed types of nanostructures, their morphology and crystal structure are, in general, consistent with the results of previous studies devoted to growing InAs nanostructures via the VLS and VSS mechanisms on substrates of other types [1,6–8]. The exception are peculiarities of NWs growing in the $[110]$ direction, which manifest themselves in formation of a non-planar catalyst–NW interface (Fig. 2). Previously it was reported that, in the case of the VLS growth of InAs NWs in the given direction, the interface has only one facet, namely $[\bar{1}\bar{1}\bar{1}]$ [7]. The non-planar character of the catalyst–NW interface geometry revealed in our study means that the growth mechanism of such crystals differs significantly from the well-studied mechanism of NW growth in the $[\bar{1}\bar{1}\bar{1}]/[111]$ direction. In the latter case, the source of steps growing at the catalyst–NW interface are two-dimensional islands emerging on the atomically smooth upper facet of NW during the layer-by-layer growth. When the interface is formed by two planes InAs(11 $\bar{1}$) and InAs(111), the preferable place of island nucleation is the region near the edge of the dihedral angle, since in this case the islands perimeter length is minimal at the fixed volume (Fig. 3). Notice that position of an island emerging on the edge formed by the InAs(11 $\bar{1}$) and InAs(111) planes is always consistent with the zinc blende structure. On the contrary, position of an island emerging on an atomically smooth facet, e.g. InAs(11 $\bar{1}$), is consistent with either the zinc blende or wurtzite structure. This fact explains the effect of polytypism (zinc blende/wurtzite) often observed during the growth in the $[\bar{1}\bar{1}\bar{1}]/[111]$ direction of NWs whose radii exceed $\sim 10\ \text{nm}$ [9]. Thus, the defect-free

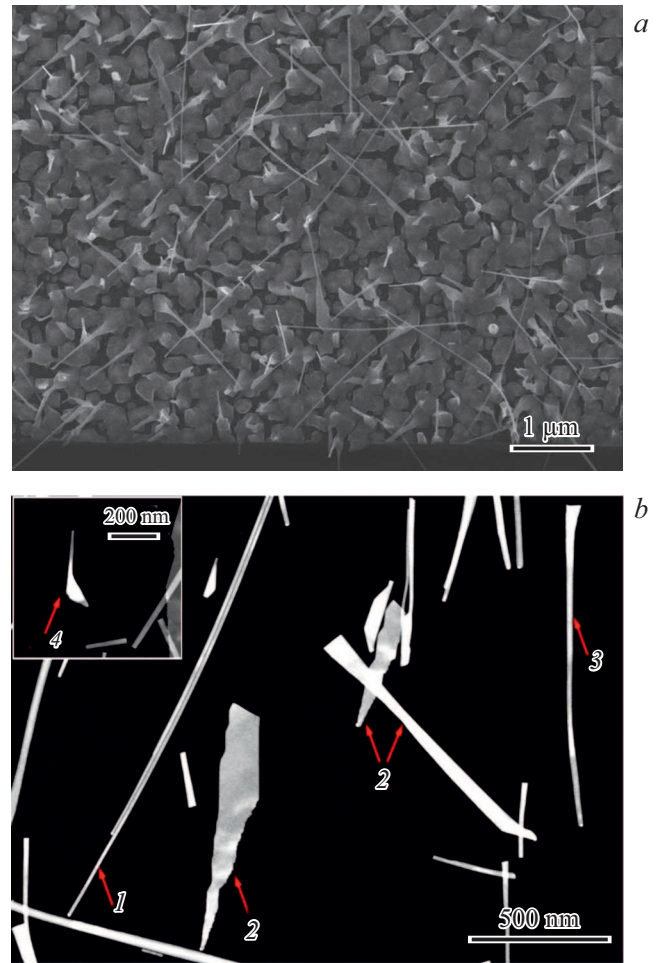


Figure 1. *a* — SEM image of an array of InAs nanostructures grown on the Si(100) substrate. *b* — TEM image of various types of nanostructures after transferring them from the substrate to the carbon grid. 1 — NWs growing in the $[000\bar{1}]$ direction; 2 — nanosheets; 3 — NWs growing in the $[110]$ direction; 4 — nanosheets arising due to instability of the catalyst particle.

structure of NWs growing in the InAs $[110]$ direction may be caused by the presence of a non-planar interface with the catalyst. Notice also that the observed (11 $\bar{1}$) and (111) facets have been earlier discovered on the A^{III}B^V semiconductor surface (110) after etching by depositing metal films and annealing [10]. However, in this case the material transport at the metal–semiconductor interface proceeds in the opposite direction. Since the InAs(11 $\bar{1}$) and InAs(111) surfaces are bounded by atoms of different types, namely arsenic and indium, respectively, the lateral growth rates of steps on these planes are different. Let us evaluate the stability of the size of these facets within the framework of the simple geometric model presented in the inset to Fig. 3. Assume that, being nucleated, an island located on the edge can grow laterally both along the InAs(11 $\bar{1}$) facet l_1 long and InAs(111) facet l_2 long at the rates of V_1 and V_2 , respectively. Let us determine the normal growth rates of the InAs(11 $\bar{1}$) and InAs(111) facets through formulae

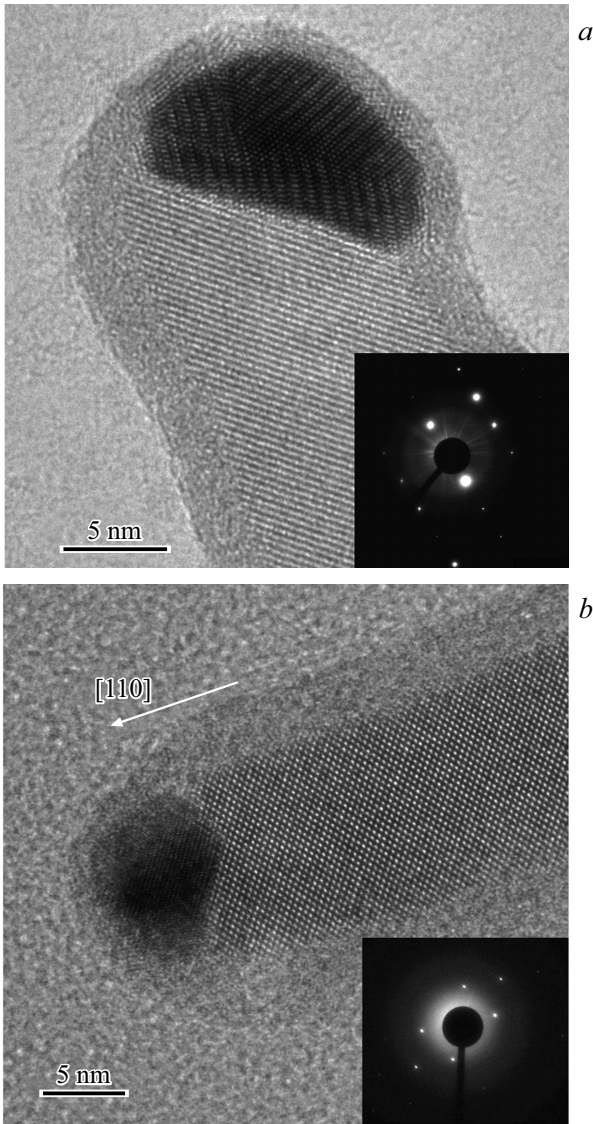


Figure 2. TEM images of the top of the InAs nanosheet (*a*) and top of the InAs NW growing in the [110] direction (*b*). The insets present diffraction patterns of the nanosheets and nanowires.

$V_{01} = hV_1/l_1$ and $V_{02} = hV_2/l_2$, where h is the monolayer height. Then the equation for the rate of variation in the first facet length l_1 takes the following form:

$$dl_1/dt = (V_{01} - V_{02})/\sin 2\alpha,$$

where t is the growth time, α is the angle between the [110] and $[1\bar{1}\bar{1}]$ directions. From this equation it follows that the condition for stationary growth of NWs is equality $V_1/V_2 = l_1/l_2$. Expressing the normal growth rates of facets in terms of lateral growth rates of the respective steps, taking into account that $l_2 = l_{\max} - l_1$, and introducing dimensionless quantities $l = l_1/l_{\max}$, $V = V_1/V_2$ and $\tau = thV_2/(l_{\max}^2 \sin 2\alpha)$, where $l_{\max} = d/\cos \alpha$, d is the NW diameter, obtain a differential equation defining the

length of the first facet:

$$\frac{dl}{d\tau} = \frac{V - (1+V)l}{l(1-l)}. \quad (1)$$

Integrating equation (1) with initial condition $l(0) = l_0$, find the solution in the form of inverse function

$$\tau = \frac{(l-l_0)(1+V)((l+l_0)(1+V)-2) - 2V \ln\left(\frac{l(1+V)-V}{l_0(1+V)-V}\right)}{2(1+V)^3}, \quad (2)$$

where $l \geq V/(1+V)$ ($l \leq V/(1+V)$) provided $l_0 > V/(1+V)$ ($l_0 < V/(1+V)$). As shown by the function $l(\tau)$ curves (Fig. 3) plotted for different values of initial facet length l_0 , this solution is stable. With increasing time, the facet size l tends to a stationary value according to the following formula (the stationary growth condition in the dimensionless form):

$$l = \frac{V}{1+V}. \quad (3)$$

Assuming that growth on the InAs(11 $\bar{1}$) facet is faster than on the InAs(111) facet [7], find from the TEM image shown in Fig. 2, *b* that $l \sim 0.6$. Then obtain from equation (3) the ratio between the growth rates of the InAs(11 $\bar{1}$) and InAs(111) facets; it appears to be $V \sim 1.5$. It is important to notice that, due to the stationary growth condition, the NW top will retain both facets even if the difference in step velocities on these facets is relatively large.

Thus, in this work we have studied the MBE growth of InAs nanostructures on Si(100) substrates via the VSS mechanism. The morphology and crystal structure of nanowires and nanosheets formed on these substrates have been examined. It was found out that, when NWs grow

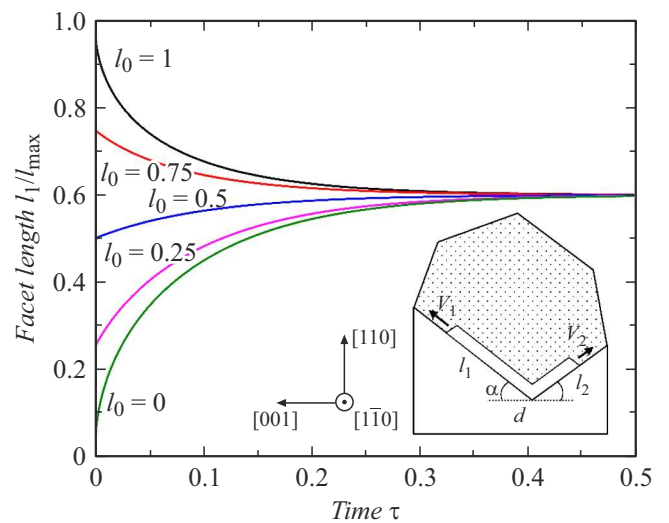


Figure 3. Relative length $l = l_1/l_{\max}$ of the facet located at the catalyst–NW interface versus the growth time at different initial lengths l_0 and ratio $V_1/V_2 = 1.5$ between the facet growth rates. The inset presents the model geometry of the top of NW growing in the [110] direction.

in the InAs[110] direction, the catalyst–NW interface is not flat. A model was proposed within which the stability of facets constituting the interface was studied.

Funding

Experimental samples were grown under the financial support of the Ministry of Science and Higher Education of the Russian Federation (№ 075-01157-23-00, topic FFZM-2022-0008). Morphological and structural properties of the grown samples were studied by using the equipment of the Saint Petersburg State University Interdisciplinary Resource Center „Nanotechnology“ under the support of Saint Petersburg State University, project code 95446496. Theoretical calculations were supported by the Ministry of Science and Higher Education of the Russian Federation (0791-2023-0004).

Conflict of interests

The authors declare that they have no conflict of interests.

References

- [1] Q. Sun, H. Gao, X. Zhang, X. Yao, S. Xu, K. Zheng, P. Chen, W. Lu, J. Zou, *Nanoscale*, **12** (1), 271 (2020). DOI: 10.1039/C9NR08429K
- [2] C.B. Maliakkal, M. Tornberg, D. Jacobsson, S. Lehmann, K.A. Dick, *Nanoscale Adv.*, **3** (20), 5928 (2021). DOI: 10.1039/D1NA00345C
- [3] V.G. Dubrovskii, *Nanomaterials*, **11** (9), 2378 (2021). DOI: 10.3390/nano11092378
- [4] S.E.R. Hiscocks, W. Hume-Rothery, *Proc. R. Soc. Lond. A*, **282** (1390), 318 (1964). DOI: 10.1098/rspa.1964.0235
- [5] R.R. Reznik, G.E. Cirlin, I.V. Shtrom, A.I. Khrebtov, I.P. Soshnikov, N.V. Kryzhanovskaya, E.I. Moiseev, A.E. Zhukov, *Tech. Phys. Lett.*, **44** (2), 112 (2018). DOI: 10.1134/S1063785018020116.
- [6] A.A. Koryakin, S.A. Kukushkin, K.P. Kotlyar, E.D. Ubyivovk, R.R. Reznik, G.E. Cirlin, *CrystEngComm*, **21** (32), 4707 (2019). DOI: 10.1039/C9CE00774A
- [7] Z. Zhang, Z. Lu, H. Xu, P. Chen, W. Lu, J. Zou, *Nano Res.*, **7** (11), 1640 (2014). DOI: 10.1007/s12274-014-0524-x
- [8] A. Kelrich, O. Sorias, Y. Calahorra, Y. Kauffmann, R. Gladstone, S. Cohen, M. Orenstein, D. Ritter, *Nano Lett.*, **16** (4), 2837 (2016). DOI: 10.1021/acs.nanolett.6b00648
- [9] T. Akiyama, K. Sano, K. Nakamura, T. Ito, *Jpn. J. Appl. Phys.*, **45** (9), L275 (2006). DOI: 10.1143/JJAP.45.L275
- [10] J.W. Faust, A. Sagar, H.F. John, *J. Electrochem. Soc.*, **109** (9), 824 (1962). DOI: 10.1149/1.2425562

Translated by EgoTranslating